Acoustics'08 Paris
June 29-July 4, 2008
www.acoustics08-paris.org

Singing Integrals or wind instruments modeling using Boundary Integral Equations

Umberto Iemma

University Roma Tre, via vasca navale 79, 00146 Rome, Italy
u.iemma@uniroma3.it

The paper deals with the modeling of woodwind musical instruments using a Boundary Integral Equation (BIE) formulation. Specifically, the BIE is used to model the acoustic response of the instrument bore, and is numerically solved by means of a Boundary Element Method (BEM). The latter takes advantage of an analytical solution for the calculation of the BEM coefficients, thus allowing for the representation of the problem as an open-domain problem. This peculiarity avoids the use of approximated boundary conditions at the open end of the pipe. The formulation is used to: evaluate the input impedance of the resonating air column; evaluate the time–domain "reflection coefficient"; identify the frequency dependent transfer function relating the inflow of the instrument with the signal at observation points in the field (the "Reed-To-Microphone" transfer function); extend the analysis to a realistic performing environment to obtain the "Reed-To-Listener" transfer function. Standard techniques are used to take into account the interaction of the bore with the nonlinear exciting device. Numerical results are obtained for single-reed instruments in terms of tuning properties, convergence of solution, directivity patterns, and simple synthesized sounds. Issues related to the possibility of real-time simulations are briefly addressed. Specifically, the identification of digital filters from the calculated transfer functions is investigated, and some preliminary numerical result included.

1 Introduction

A numerical tool capable to predict reliably the acoustic response of a wind musical instrument is highly desirable, not only as a support to instruments design, but also for sound synthesis purposes. Unfortunately, most of the numerical methods available for the solution of acoustic problems fail to give reliable results in this kind of applications. The main reason for this resides in the difficulties arising in the modeling of the boundary conditions associated to this class of problems. Indeed, at the open of the pipe part of the energy associated with the wave traveling inside the instrument is radiated into the outer domain, whereas the remaining part is reflected back in the instrument bore. This energy balance is governed by the geometry of the output section of the instrument, and the appropriate conditions to be applied to model it, are not easy to derive. When approaching the problem using standard simulation methods the wave evolution inside the instrument bore and the sound propagation in the surrounding environment are typically considered as two distinct problems. The two domains are connected through a fictitious boundary, on which approximated boundary conditions are applied. The accuracy of such an approach is poor when a realistic flare geometry is considered, due to the intrinsic uncertainties in the definition of the fictitious boundary. Here, the problem is circumvented by modeling the problem in a fashion as close as possible to the real world. Indeed, the air column enclosed by the instrument body is considered as a part of the complete acoustic domain where the sound waves are allowed to propagate (as it really is!). Using this approach there is no need of dedicated boundary conditions at the output section of the instrument, and the evolution of the wave system in all the available space is modeled as a whole. The method is applied to the prediction of the tuning properties of clarinet and saxophones, as well as to the evaluation of their directivity patterns. In addition, preliminary sound are synthesized by including a simple interaction scheme with the reed/mouthpiece system.

2 The Boundary Integral Equation

The propagation of a small–amplitude acoustic perturbation within an inviscid, non-conducting, compressible medium at rest, can be described by the velocity potential $\varphi(\mathbf{x}, t)$, assumed that no vorticity sources are present in the field. The equation governing the propagation of the potential waves in the domain $\mathcal{V}$, written in the frequency domain, is the Helmholtz equation,

$$\nabla^2 \tilde{\varphi} + k^2 \, \tilde{\varphi} = 0, \qquad \forall \mathbf{x} \in \mathcal{V} \tag{1}$$

where the wave number k is the ratio between the angular frequency ω and the speed of sound c, and the $\tilde{}$ indicates the Fourier transform. The pressure perturbation can be extracted from the potential through the linearized Bernoulli's theorem

$$\tilde{p} - \tilde{p}_0 = -j\omega \, \varrho \, \tilde{\varphi}, \tag{2}$$

where ϱ is the air density, and $\tilde{p}_0$ is the reference pressure. The above problem is completed by the boundary conditions on $\partial\mathcal{V}$, which will be discussed in detail in Section 3. The boundary value problem so obtained can be recast in an integral form using the standard procedure (see, *e.g.*, [5]), to yield

$$E(\mathbf{y})\tilde{\varphi}(\mathbf{y}) = \oint_{\mathcal{S}} \left(G \frac{\partial \tilde{\varphi}}{\partial n} - \tilde{\varphi} \frac{\partial G}{\partial n} \right) d\mathcal{S}(\mathbf{x}). \tag{3}$$

Here, $G(\mathbf{x}, \mathbf{y}, k) = -e^{-jkr}/4\,\pi\,r$ is the free–space Green's function for the three–dimensional wave operator, $r = |\mathbf{x} - \mathbf{y}|$ is the distance between the source point $\mathbf{x} \in \mathcal{S}$ and the observation point $\mathbf{y} \in \overline{\mathcal{V}}$ (with $\overline{\mathcal{V}} = \mathcal{V} \cup \partial\mathcal{V}$). The domain function $E(\mathbf{y}) = 1$ if $\mathbf{y} \in \mathcal{V}$ and $E(\mathbf{y}) = 1/2$ if $\mathbf{y} \in \partial\mathcal{V}$. This equation is formally identical to the classic Kirchhoff–Helmholtz integral theorem, written in terms of the velocity potential function $\tilde{\varphi}$. Note that, if $\tilde{\varphi}$ and $\partial\tilde{\varphi}/\partial n$ are known on the boundary of $\mathcal{V}$, then Eq. 3 may be used as a direct representation of $\tilde{\varphi}$ at an arbitrary location $\mathbf{y} \in \mathcal{V}$. On the other hand, when the Cauchy data set associated to the problem are not completely known (see Section 3) the problem can be solved by locating the observation point $\mathbf{y}$ on $\mathcal{S}$. In this case, Eq. 3 assumes the role of a compatibility condition between the velocity potential function and its normal derivative, and can be numerically solved using the boundary element method, as explained in Section 4. In order to use this integral formulation to simulate the acoustic response of a wind instrument, it is necessary to clearly define the domain $\mathcal{V}$, its boundary $\mathcal{S} = \partial\mathcal{V}$, and the boundary conditions on it.

3 The boundary conditions

The physical phenomenon under analysis deals essentially with the evolution of the wave system induced inside the instrument bore by the interaction of the exciting device (the reed/mouthpiece system, in our case) with the air column. At the open end, the forward–traveling wave partially radiates outside, and the reflected wave travels back into the duct with a reduced energy content. When the backward wave reaches the mouthpiece, the amount of energy radiated in the surrounding environment is restored by the exciting device, which is fed by the pressure reservoir represented by the players breathing system. A correct reproduction of this mechanism requires an accurate modeling of the radiation properties at the open end (see *e.g.*, [2]). This is not an easy task, especially for the complex geometries typical of the musical instruments. In this work, the resonating air column is considered as a part of the whole acoustic domain, reproducing as close as possible the real world conditions. The resulting domain where Eq. 1 is to be solved is presented in Figure 1. The domain $\mathcal{V}$ is the union of the interior of the pipe, $\mathcal{V}_{\mathsf{int}}$ and the external open space $\mathcal{V}_{\mathsf{out}}$. The body of the instrument has a (non–physical) thickness, so as to ensure the applicability of the integral formulation presented. The domain boundary is given by $\partial\mathcal{V} = \mathcal{S}_{\mathsf{in}} \cup \mathcal{S}_{\mathsf{p}} \cup \mathcal{S}_\infty$, where $\mathcal{S}_{\mathsf{in}}$ represent a fictitious surface introduced at the input section of the pipe (the need for this surface will be clarified later), whereas $\mathcal{S}_{\mathsf{p}}$ is the surface of the instrument pipe, and $\mathcal{S}_\infty$ is the boundary at infinite distance. The boundary conditions of the problem in their more general form, derive from the relationship that holds on $\partial\mathcal{V}$ between the velocity potential and the normal acoustic velocity

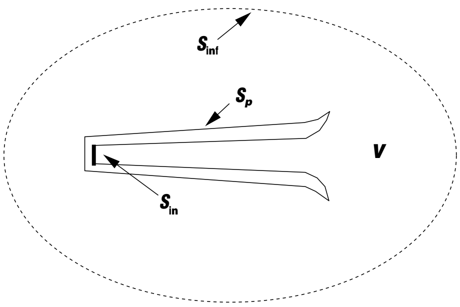

Figure 1: Domain boundary

$$\alpha(\mathbf{x},k)\,\tilde{\varphi}(\mathbf{x},k) + \beta(\mathbf{x},k)\,\frac{\partial\tilde{\varphi}}{\partial n}(\mathbf{x},k) = f(\mathbf{x},k), \qquad (4)$$

where α, β and f are, in general, complex functions of position and frequency, and $\partial\tilde{\varphi}/\partial n = \nabla\tilde{\varphi}\cdot\mathbf{n}$. In our case, the specific conditions to be applied on each partition of the boundary are:

- the acoustic impermeability of instrument walls, $\mathcal{S}_{\mathsf{p}}$ $(\alpha = f = 0,\ \beta = 1)$

$$\frac{\partial\tilde{\varphi}}{\partial n} = 0 \qquad\qquad \mathbf{x}\in\mathcal{S}_{\mathsf{p}}; \qquad (5)$$

- the prescribed input velocity $\mathbf{v}_{\mathsf{in}}(\mathbf{x})$ on the input section $\mathcal{S}_{\mathsf{in}}$ $(\alpha = 0,\ \beta = 1,\ f = \mathbf{v}_{\mathsf{in}}\cdot\mathbf{n})$

$$\frac{\partial\tilde{\varphi}}{\partial n} = \mathbf{v}_{\mathsf{in}}(\mathbf{x})\cdot\mathbf{n} \qquad\qquad \mathbf{x}\in\mathcal{S}_{\mathsf{in}}. \qquad (6)$$

In addition, the Sommerfeld radiation condition implies $\tilde{\varphi} = \mathcal{O}(r^{-1})$ for $\mathbf{x}\to\mathcal{S}_\infty$. Hence, in Eq. 3, $\mathcal{S} = \mathcal{S}_{\mathsf{in}}\cup\mathcal{S}_{\mathsf{p}}$.

4 The BEM

To numerically solve the problem, the Boundary Element Method (BEM) is used. The boundary of the domain is partitioned into N quadrilateral panels. All the quantities are considered to be constant within each panel (*zeroth–order* approximation). The surface integral in Eq. 3 is approximated with a sum of N panel integrals, and the collocation method is used, by locating the collocation points at the centers of the panels. The discrete approximation of Eq. 3 is

$$\frac{1}{2}\,\tilde{\varphi}(\mathbf{x}_n,k) = \sum_{m=1}^{N}\left[B_{nm}\,\frac{\partial\tilde{\varphi}}{\partial n}(\mathbf{x}_m,k) + C_{nm}\,\tilde{\varphi}(\mathbf{x}_m,k)\right] \quad (7)$$

for $\mathsf{n} = 1,\ldots,N$, and

$$B_{nm} = \int_{\mathcal{S}_m} G(\mathbf{x}_m,\mathbf{x}_n,k)\,dS, \qquad (8)$$

$$C_{nm} = \int_{\mathcal{S}_m} \frac{\partial G(\mathbf{x}_m,\mathbf{x}_n,k)}{\partial n}\,dS. \qquad (9)$$

Taking advantage of the zeroth–oder formulation, the coefficients 8 can be evaluated analytically (see [6]). Collecting the integral coefficients in Eq. 8 into the $[N\times N]$ complex matrices B and C, and the value of the velocity potential and its normal derivative respectively into the $[N\times 1]$ column vectors $\underline{\tilde{\varphi}}$ and $\underline{\tilde{\chi}}$, the solution of the system in matrix form is

$$\underline{\tilde{\varphi}} = \mathsf{Y}^{-1}\,\mathsf{B}\,\underline{\tilde{\chi}}, \qquad \text{with } \mathsf{Y} = \left(\frac{1}{2}\,\mathsf{I} - \mathsf{C}\right), \qquad (10)$$

being $\underline{\tilde{\chi}}$ known from the boundary conditions.

5 Modeling the instrument

The formulation outlined so far is used to model the acoustic response of the instrument. In the following, the approach used is briefly described in specific subsections, each dedicated to one of the aspects taken into account.

5.1 The input impedance

The input impedance $\mathcal{Z}_{\mathsf{in}}$ of the bore is a crucial parameter to characterize the acoustic properties of the instrument. $\mathcal{Z}_{\mathsf{in}}$ is defined as the ratio between the pressure jump existing across the input section $\mathcal{S}_{\mathsf{in}}$, and the resulting acoustic flow,

$$\mathcal{Z}_{\mathsf{in}}(k) = \frac{\tilde{p} - \tilde{p}_0}{\mathbf{v}_{\mathsf{in}} \cdot \mathbf{n}}. \tag{11}$$

The input impedance varies greatly with frequency and its maxima and minima correspond to the frequencies at which a steady wave system can be established within the bore through the interaction with the exciting device. In other words, $\mathcal{Z}_{\mathsf{in}}(k)$ identifies the basic tuning of the instrument. Here, the input impedance is considered as the transfer function between the inflow and the pressure perturbation. It is evaluated by imposing a harmonic input velocity at $\mathcal{S}_{\mathsf{in}}$ with frequency spanning the whole range of interest with a given step $\Delta\omega$. The solution is then calculated with Eq. 10, and $\mathcal{Z}_{\mathsf{in}}$ is obtained through

$$\mathcal{Z}_{\mathsf{in}}(\omega_{\mathsf{i}}) = \frac{-1}{\mathcal{S}_{\mathsf{in}}} \int_{\mathcal{S}_{\mathsf{in}}} \frac{\tilde{p} - \tilde{p}_0}{\mathbf{v}_{\mathsf{in}} \cdot \mathbf{n}} \mathrm{d}\mathcal{S} \simeq \frac{-1}{\mathcal{S}_{\mathsf{in}}} \sum_{m=1}^{N_{\mathsf{in}}} j\omega_{\mathsf{i}}\, \rho\, \frac{\tilde{\varphi}_{\mathsf{m}}}{\tilde{\chi}_{\mathsf{m}}}\, s_{\mathsf{m}} \tag{12}$$

where N_{in} is the number of panels on $\mathcal{S}_{\mathsf{in}}$, and s_{m} represents the area of the $m-$th panel.

5.2 The reflection coefficient

The interaction of the exciting device (the reed in woodwinds, the jet for flutes, or the player's lips for brasses) with the resonating air column should be typically performed in the time domain, due to intrinsic nonlinearity of the pressure-flow relationships (see [4]). The resulting convolution converges extremely slowly, due to the richness of the $\mathcal{Z}_{\mathsf{in}}$ spectrum. To circumvent this problem, we introduce the reflection function $\mathcal{R}(k)$ as the transfer function between the incoming and reflected waves at the open end of the pipe, $\tilde{p}^-(k) = \mathcal{R}(k)\tilde{p}^+(k)$ with $\tilde{p}_{\mathsf{in}} = \tilde{p}^+(k) + \tilde{p}^-(k)$. The *reflection coefficient* is the inverse Fourier transform of $\mathcal{R}$, and can be evaluated as

$$r(t) = \mathcal{F}^{-1}\left[\frac{\mathcal{Z}_{\mathsf{in}}(k) - \mathcal{Z}_0}{\mathcal{Z}_{\mathsf{in}}(k) + \mathcal{Z}_0}\right], \quad \text{with } \mathcal{Z}_0 = \frac{\varrho\, c}{\mathcal{S}_{\mathsf{in}}} \tag{13}$$

The pressure jump inside the mouthpiece can be obtained through the (rapidly converging) convolution

$$p(t) = r(t) * [p(t) + \mathcal{Z}_0 \mathbf{v}_{\mathsf{in}}(t) \cdot \mathbf{n}] + \mathcal{Z}_0 \mathbf{v}_{\mathsf{in}}(t) \cdot \mathbf{n}.$$

5.3 Reed–To–Microphones ($\mathsf{R_2M}$) Transfer Function

The formulation presented may be used to derive a matrix transfer function relating the inflow $\mathbf{v}_{\mathsf{in}} \cdot \mathbf{n}$ to the pressure evaluated at arbitrary locations in the field. Indeed, indicating with $\underline{\tilde{\varphi}}^{\mathsf{M}}$ the column matrix collecting the value of the velocity potential at M observation points in the field (the *microphones*), the pressure at the same locations is given by $\underline{\tilde{p}}^{\mathsf{M}} = -j\omega\, \varrho\, \underline{\tilde{\varphi}}^{\mathsf{M}}$. Applying the BEM approach described above to obtain the value of $\underline{\tilde{\varphi}}^{\mathsf{M}}$ yields

$$\underline{\tilde{\varphi}}^{\mathsf{M}} = \mathsf{B}^{\mathsf{M}}\, \underline{\tilde{\chi}} + \mathsf{C}^{\mathsf{M}}\, \underline{\tilde{\varphi}} \tag{14}$$

where the entries of the $(M \times N)$ matrices B^{M} and C^{M} are the integral coefficients describing the influence of the N panels at the M external microphones. Substituting Eq. 10 into Eq. 14, and recalling the linearized Bernoulli's equation, the relationship between $\underline{\tilde{\chi}}$ and $\underline{\tilde{p}}^{\mathsf{M}}$ is

$$\underline{\tilde{\mathsf{p}}}^{\mathsf{M}} = -j\,\omega\,\varrho\, \left(\mathsf{B}^{\mathsf{M}} + \mathsf{C}^{\mathsf{M}}\,\mathsf{Y}^{-1}\mathsf{B}\right) \underline{\tilde{\chi}} = \mathsf{R_2M}(k)\, \underline{\tilde{\chi}} \tag{15}$$

where the $(M \times N)$ frequency–dependent matrix $\mathsf{R_2M}$ is the desired reed–to–microphones transfer function. The described approach is applied to evaluate the directivity pattern of the instrument, by locating the microphones along a circle centered on the instrument output section.

6 Numerical results

The method presented has been applied and validated in a number of preliminary test cases, involving simple straight geometries (soprano saxophones and clarinets). The effect of tuning holes has not been taken into account. First, the evaluation of the input impedance has been validated against the well-assessed method of Levine and Schwinger [1], for a cylindrical pipe 1 meter long, with an internal radius of 1 cm. The dimensionless ratio $\mathcal{Z}_{\mathsf{in}}(k)/\mathcal{Z}_0$ is presented in Fig. 2. The agreement between the present method and the reference is excellent along the whole frequency range considered. The convergence analysis of the position of the first peak shows a remarkable agreement of the asymptotic solution with the reference. The method is then applied to the real geometries of a clarinet and a soprano saxophone (see, for details, [3]). In both cases, the frequency where the $\mathcal{Z}_{\mathsf{in}}$ spectrum presents the first peak corresponds exactly to the frequency of the lowest playable tone (D_3 for the clarinet and $A_3^\flat$ for the sax, Figures 4, 5). Note that the cylindrical profile of the clarinet bore produces a $\mathcal{Z}_{\mathsf{in}}$ spectrum including only the odd harmonics of the fundamental, whereas the conical section of the sax generates a complete harmonic series.

In order to validate the method for a more complicated geometry, the frequency shift of the fundamental in presence of a curved bore has been predicted for the elbow of a tenor saxophone. The resulting spectrum is presented in Figure 6, and compared to the one obtained for an equally long straight tube, as well as with the prediction of a standard semi-empirical correction formula. The prediction of the present method is in good agreement with the latter, revealing that the formulation is capable to capture the effects of more complicated instrument profiles.

The directivity pattern of a soprano saxophone is presented in Figure 7. Even if a reference solution for the validation of the result is not available, the polar plot appears to be consistent with the expected intensity distribution for the three frequencies analyzed.

The following results deal with the synthesis of the sound produced by simulating the interaction of the resonating air column with the reed/mouthpiece for the same instruments of the previous tests. The model used for the reed is that of a simple pressure–driven valve (see [4] and [3]), and is coupled to the instrument bore through the convolution of the reflection coefficient (see Figure 8) with the pressure signal inside the mouthpiece. The inflow and the pressure signals at the input section of the clarinet are depicted in Figures 9 and 10. The time–marching procedure reaches a steady state corresponding to the correct frequency (the one of the lowest playable tone), and the "almost square" pressure profile fits well with the oscillation pattern observed inside a clarinet mouthpiece (see [4]).

Finally, a preliminary attempt to obtain a binaural sound signal at the location of a virtual listener is presented in Figure 11. The approach presented in Section 5.3 has been extended to take into account the presence of the listener body, and its effect on the sound propagation (the derivation of the resulting matrix transfer function is not included here for the sake of conciseness). The time signal at the location corresponding to the listener ears appear to be correctly shifted in amplitude and phase. The audio effect can be considered as good, considering the rough approximations of the model.

References

[1] H. Levine, J. Schwinger, On the radiation of sound from an unflanged pipe, Physics Review 73 (1948) 383–406.

[2] J.-P. Dalmont, C. J. Nederveen, N. Joly, Radiation impedance of tubes with different flanges: Numerical and experimental investigations., Journal of Sound and Vibration 244 (2001) 505–534.

[3] C. J. Neederveen, Acoustical Aspects of Woodwind Instruments, De Kalb - Northern Illinois, 1969, revised edition 1998.

[4] N. H. Fletcher, T. D. Rossing, The Physics of Musical Instruments, Springer–Verlag, New York, 1991.

[5] A. D. Pierce, Acoustics - An Introduction. Its Physical Principles and Applications, Acoustical Society of America, New York, 1989.

[6] U. Iemma, Boundary Integral Equation Methods for Transonic Flows, Phd thesis, University of Roma *La Sapienza* (1994) (in italian).

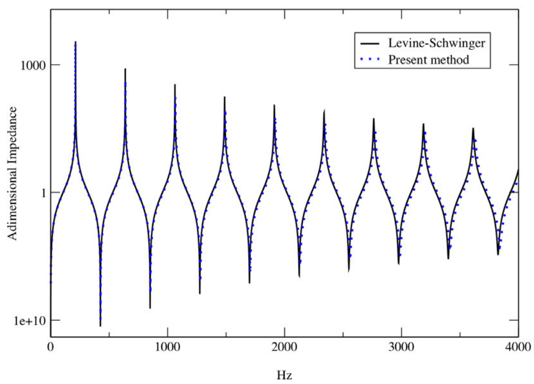

Figure 2: Dimensionless input impedance for a cylindrical tube ($L = 1\,m.$, $r = 1\,cm.$). Comparison with the Levine & Schwinger theory.

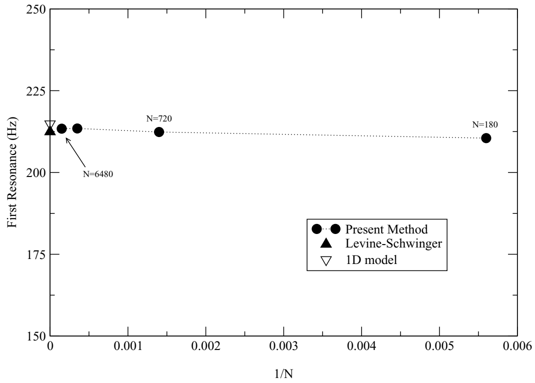

Figure 3: Convergence of the first impedance peak w.r.t. the number of boundary elements.

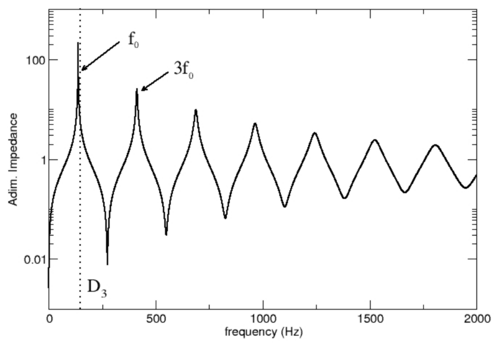

Figure 4: Dimensionless input impedance for a clarinet.

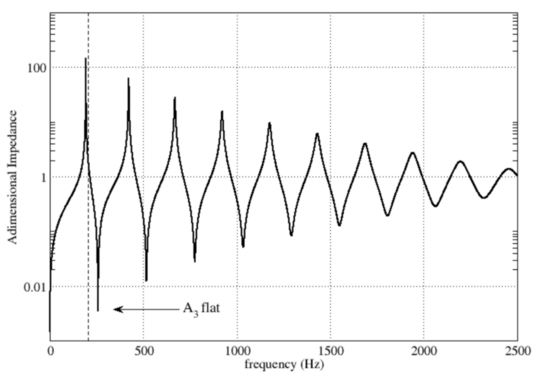

Figure 5: Dimensionless input impedance for a soprano saxophone.

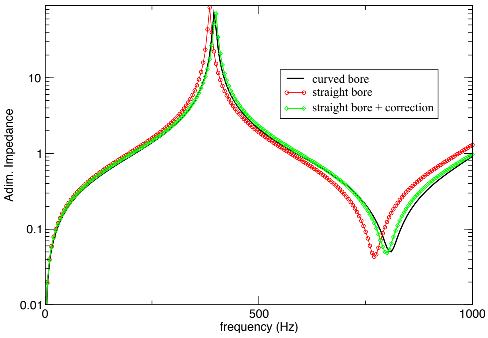

Figure 6: Effect of the curvature for the elbow of a tenor saxophone.

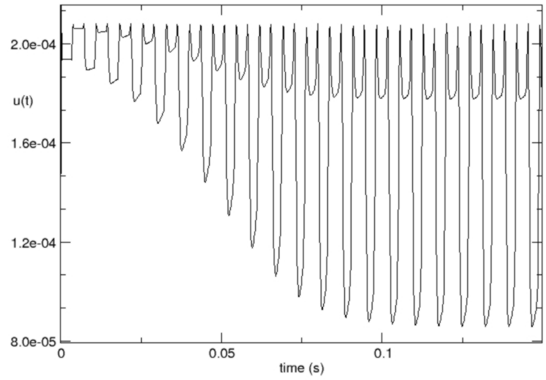

Figure 9: Clarinet inflow in playing condition. Lowest tone.

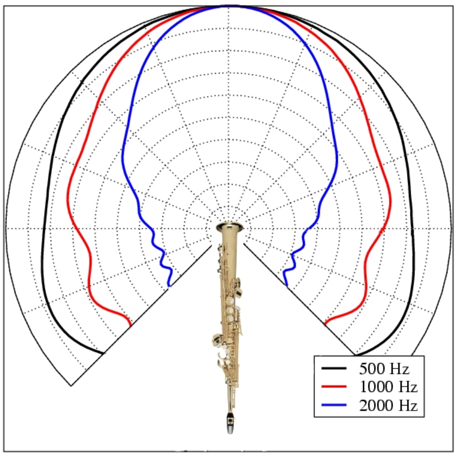

Figure 7: Directivity pattern of a soprano saxophone.

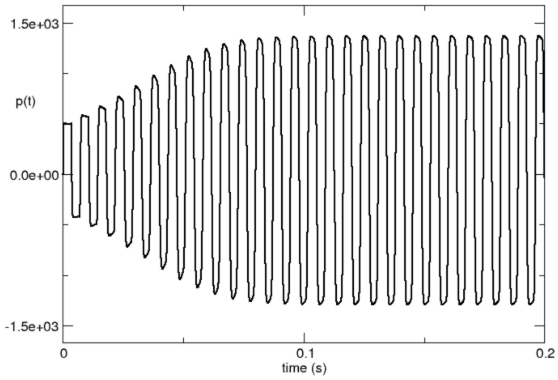

Figure 10: Pressure at the clarinet input section in playing condition. Lowest tone.

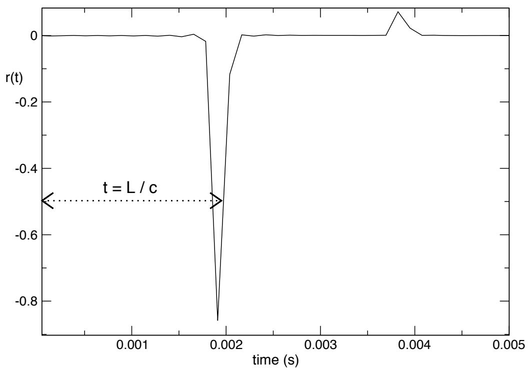

Figure 8: Reflection coefficient calculated from the $\mathcal{Z}_{\text{in}}$ in Fig. 4.

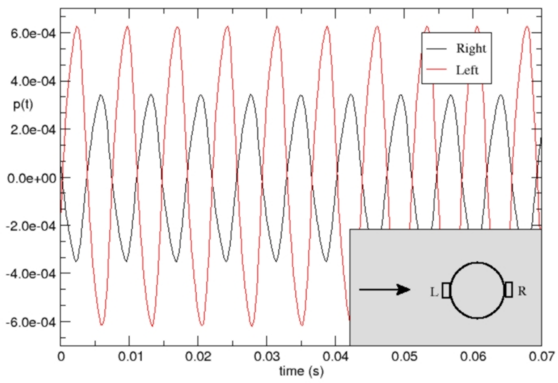

Figure 11: Clarinet sound perceived at the listener location.